Experimental Investigation of Water-Based Fire Suppression Systems on External Façade Fires

Christoph Meraner (ID)*, *Ellen S. Skilbred* and *Kemal S. Arsava, RISE Fire Research, Trondheim, Norway*

Abstract. The use of external fire suppression systems can reduce the risk of fire spreading between buildings. This study investigated the effectiveness and efficiency of different externally placed water-based fire suppression systems on façade fire safety. A series of large-scale experiments comprising an SP Fire 105 setup equipped with sprinklers and high-pressure water mist nozzles have been performed. A combustible façade, consisting of 2.5 cm thick oriented strand board (OSB) plates, was installed to provide challenging conditions and allow a visual assessment of the post-fire damage. The temperature profile on the façade surface was measured with 34 thermocouples, while five heat flux gauges and two fast-response plate thermocouples were used to measure the heat flux on the façade surface and emitted to the ambient. The sprinklers and the high-pressure water mist system effectively suppressed the upwards flame migration and reduced the heat flux toward adjacent buildings. It was observed that the sprinklers acted as a water curtain and kept the façade wet during the fire, promoting minor damage (the burnt area is less than 1% of the total area). The temperature and heat flux measurements demonstrated that the sprinkler system was the most effective suppression system. However, the high-pressure water mist systems achieved similar effectiveness but a much higher efficiency concerning water consumption. The sprinkler nozzles used four times as much water as the high-pressure water mist nozzles.

1. Introduction

Fire suppression systems for façades can mitigate the risk of fire spreading between levels within one building and between buildings and secure escape routes in the event of a fire. The fixed suppression systems are installed with a locked position and orientation of injection points and nozzles to promote effective suppression at specific locations. The most common fixed suppression system for façades is the façade water sprinkler system. The system can be installed on selected façades, parts of the façades or all of the façades, depending on whether the goal is to completely extinguish the fire or to prevent fires from spreading.

---

*Correspondence should be addressed to: Christoph Meraner, E-mail: christoph.meraner@risefr.no

The effects of sprinkler systems on the suppression of façade fires have been investigated in a few studies. In particular, large-scale experimental studies have been conducted to address the ability of internal sprinkler systems to protect exterior glass façades and windows [1–3]. An alternative to traditional sprinkler systems is water mist systems, which have smaller water droplets (less than 1000 μm in diameter [4]) than the sprinklers. Smaller droplets absorb heat more effectively than larger droplets due to the high surface-to-volume ratio and contribute more significantly to radiation attenuation [5–7]. Therefore, a water mist system usually needs less water than a sprinkler system for fire suppression. When comparing the performance of different water spray systems, effects such as evaporation, droplet inertia, and surface and flame cooling should also be considered [6]. Smaller droplets hover longer due to buoyancy forces compared to larger droplets, which fall fast to the ground, and the smaller droplets are therefore available to attenuate the radiation in the area where they are distributed for a longer time than the larger droplets [7] and are more effective at bypassing obstacles [8]. However, the smaller droplets are also more affected by the airflow and can be directed away from the area they are intended to protect. This is especially important on exterior façades, which are exposed to wind. Also, the larger droplets may form streams of water running down a façade or streams of water on the ground, which can cool or extinguish flames.

This study investigates the efficiency of water mist and sprinkler systems in mitigating the fire load generated by external flames on the façade and other buildings. Tests were conducted on a façade with and without suppression by sprinklers or water mist. Three different systems were investigated:

– Three sprinkler nozzles aiming to cover most of the façade's surface
– Three high-pressure water mist nozzles aiming to cover most of the façade's surface
– A single high-pressure water mist nozzle close to the combustion chamber, where the air entrainment into the flame is stronger than the wind force.

An external suppression system can be especially relevant for older buildings constructed with non-fire-resistant materials and components. In two of the water mist suppression tests, plates were placed over the nozzles to investigate if the plates would change the flow of the droplets and make them hover for a longer time, hence attenuating the radiation more effectively. The objective is to understand (1) the influence of fire loads on heat exposure of the façades and (2) the effect of different water mist/sprinkler systems on heat exposure of the façades and neighbouring buildings.

2. Experiments

2.1. Experimental Setup

Five tests were conducted in RISE Fire Research's facility in Norway. RISE Fire Research maintains a 36 m × 16 m × 22 m indoor fire hall, which allows to per-

form large-scale fire experiments in a controlled environment. The experimental test setup is based on SP Fire 105 [9], a test method used to evaluate the material's reaction to fire and fire spread from floor to floor via external walls for different wall assemblies, claddings, or insulations. The dimensions of the experimental setup are given in Figure 1. The fuel in this test method consists of 60 L heptane burning in a tray (2 m × 0.5 m × 0.1 m), stabilising the flames. This corresponds to a fire load of approximately 75 MJ/m^2 for the given burn tray.

The surface of the façade was covered with 2.5 cm thick OSB boards to visually assess the post-fire damage. The fire suppression systems were installed on the OSB surface (Figure 1).

2.2. Fire Suppression Systems

Although the basic idea of using water to suppress fire is straightforward, the suppression mechanisms of sprinklers and Water Mist (WM) are different. Sprinkler systems use larger droplets to penetrate the fire plume and cool the fuel surface directly, while WM systems reduce the flame temperature by promoting effective water evaporation, depleting the oxygen and enhancing radiative cooling by fine water droplets.

In façade fires where the flames initially eject from openings, the suppression systems need to be placed considering their dominant mechanism. Pendant sprinklers can be used on facades, but the amount of water hitting the façade will be reduced, and larger droplets will fall without interacting with the flame. When nozzles are oriented facing outwards, the deflected water will create a water curtain on the facade and cool the fuel surface. The distance between the nozzle and façade needs to be optimised, as short distances will limit water coverage area while longer distances will reduce water fire interaction. A pendant WM nozzle is more feasible for façade fires since the droplets will both cool the façade surface and the flame due to the interaction mechanism explained above. However, the WM nozzles need to be placed further away than the sprinklers, which raises architectural concerns since aspects, such as design criteria for esthetics, must also be considered in practical applications. To minimise the visual impact of nozzles on the façade, pop-up nozzles typically used in fire protection of air hangars could be used. They stay embedded in the façade surface and extend in the event of a fire.

In this study, the type and operating water pressure of the sprinkler nozzles were determined experimentally. Different nozzle types were tested with varying water flow rates in a test setup according to ISO 6182-1 [10]. The sprinkler type, and water pressure that provided the optimum façade coverage, 4.5 m diameter in this study, were determined and used in the experiments. A VdS-approved conventional pendent sprinkler with an operating pressure of 1.8 bar (0.35 bar min–12.5 bar max) and K-factor of 80 was selected. The estimated median droplet size for the sprinkler is about 1000 μm at 1.4 bar water pressure. To minimise the interaction of water with the burning pan, the height between the nozzle and the burn chamber, and the distance to the façade surface were set at 20 and 10 cm, respectively (Figure 1).
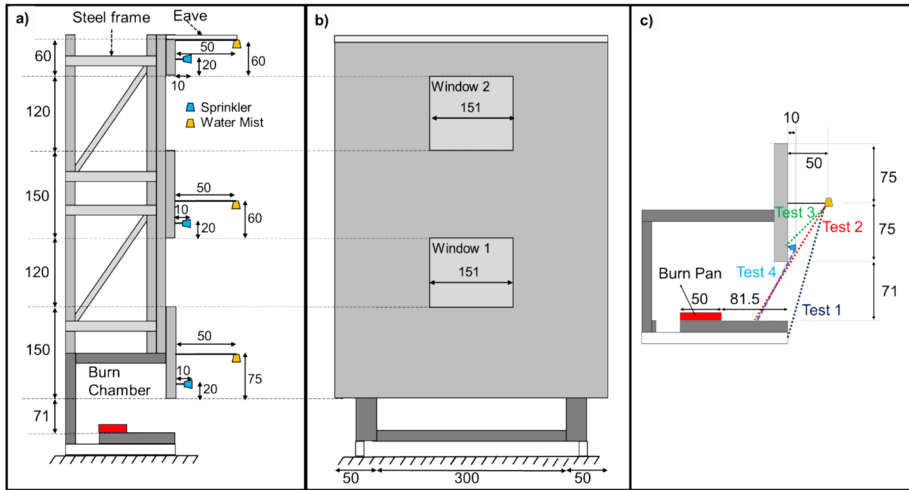
Figure 1. SP Fire 105 experimental setup equipped with sprinklers and water mist nozzles. (a) Side view, (b) Front view, (c) Scaled sketch of the burn chamber showing the water spray patterns for each test. Measurements in cm.

A spray pattern model was used to determine the location of the WM nozzles. It is observed that pendent WM nozzles with an operating pressure of 100 bar with a 90° spray angle placed 50 cm away from the façade would provide the same façade coverage as the sprinkler system and 3.5 m diameter wet area in front of the façade. Two of the nozzles (top and middle) were placed 60 cm above and 50 cm away from the top of the windows, while the third nozzle (bottom) was placed 75 cm above the burn chamber (Figure 1). The distance between the bottom nozzle and the burn chamber was kept longer to minimise the disturbance due to the proximity of the ground. The high-pressure WM nozzles used were of a commercial type, which has been large-scale fire tested for the protection of office areas, public spaces, archives, and glass partitions in accordance with EN 14972. Their K-factor is 2.75, and their pressure is 100 bar. The estimated median droplet size specified by the manufacturer for the water mist system is 90–100 μm at an operating pressure of 50 bar.

The large-scale suppression tests, which are invaluable for assessing the suppression system's real-life performance, are constrained by limitations in time and experimental matrix. Five experiments detailed in Table 1 were performed in this study. The nozzles were placed at the center of the façade to evaluate the performance of the sprinkler and water mist under similar conditions. However, authors acknowledge that further research is required to investigate the impact of different droplet sizes, flow rates, and nozzle configurations on suppression efficiency.

After the first test, 30 cm × 30 cm thin plates were installed 7.5 cm above the nozzles to improve the droplet distribution by widening the spray angle (Figure 2b). It is observed that the distance between the plate and the nozzle was not
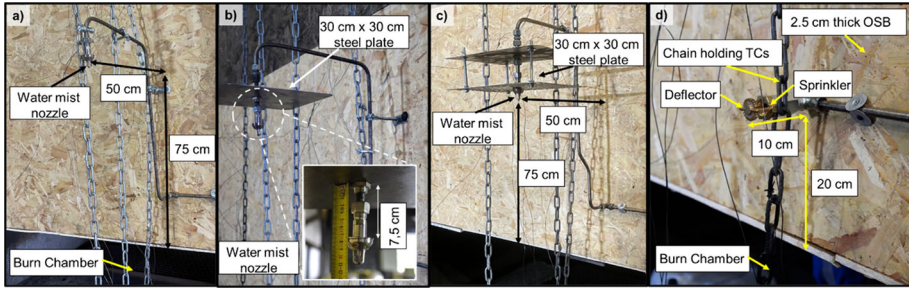
Table 1
Experimental Matrix

Test #	Nozzle type	Pressure (bar)	Number of nozzles activated	Measured spray angle	Distance to burn chamber (cm) (Figure 1a)	Top plate and distance to nozzle head (Figure 2c, d)	Activation time after ignition (min:sec)	Burn Duration (min:sec)
1	WM	100	3	50°	Top: 600 Middle: 330 Bottom: 75	No	11:30	29:54
2	WM	100	3	64°	Top: 600 Middle: 330 Bottom: 75	Yes–7.5 cm	8:25	26:08
3	WM	100	1	90°	Bottom: 75	Yes–0 cm	8:06	28:05
4	Sprinkler	1.8	3	55°	Top: 560 Middle: 290 Bottom: 20	No	13:14	27:55
5	N/A	–	–	–	–	–	–	19:16

Figure 2. **Fire suppression system installed on SP Fire 105 experimental setup: (a) high-pressure water mist nozzle without a top plate, (b) high-pressure water mist nozzle with a top plate placed 7.5 cm away from the nozzle head, (c) high-pressure water mist nozzle with a top plate placed directly above the nozzle head, (d) sprinkler.**

close enough to promote the desired effect. In the third test, the plate was placed directly above the nozzle, leading to a much wider spray cone (Figure 2c). In the sprinkler test, three sprinklers were installed 20 cm above and 10 cm away from top of the burn chamber and top of the windows (Figure 1). The sprinklers were installed pointing away from the façade with a deflector curved inside to ensure that the water sprays the façade (Figure 2d). The bulbs of the sprinklers and high-pressure WM nozzles were removed before the tests. The suppression system was activated manually after observing the self-ignition of smoke leaving the burn chamber.

A high-pressure water pump was used to supply the water to the high-pressure WM suppression system. The pressure on the pump and the top nozzle/sprinkler was measured to quantify the flow rate. The pressure measured for the high-pressure WM system was 100 bar, equivalent to the water flow rate of 27.4 L/min. The pressure measured for the sprinklers was 1.8 bar, corresponding to a flow rate of 107.3 L/min.

2.3. Instrumentation

The instrumentation used in the façade fire tests is shown in Figure 3. Three galvanised steel chains were used to hold the thermocouples (TCs). 34 K-type TCs with 24 AWG were used to measure the temperature of the façade. The chains were attached to the eave, 10 cm from the façade surface. The chain at the centre had 13 TCs with 0.5 cm spacing. Other chains containing 7 TCs, each with 100 cm spacing, were placed on the two sides 90 cm away from the centre. One total heat flux gauge (HFG) was placed at the centre of window 1 (Figure 3). Two plate thermocouples (PTs) were used, one next to the total HFG and one 100 cm away from the centre, to measure the heat flux on the surface (Figure 3a). One HFG and two radiometers were placed 400 cm away from the façade with different heights as shown in Figure 3b.
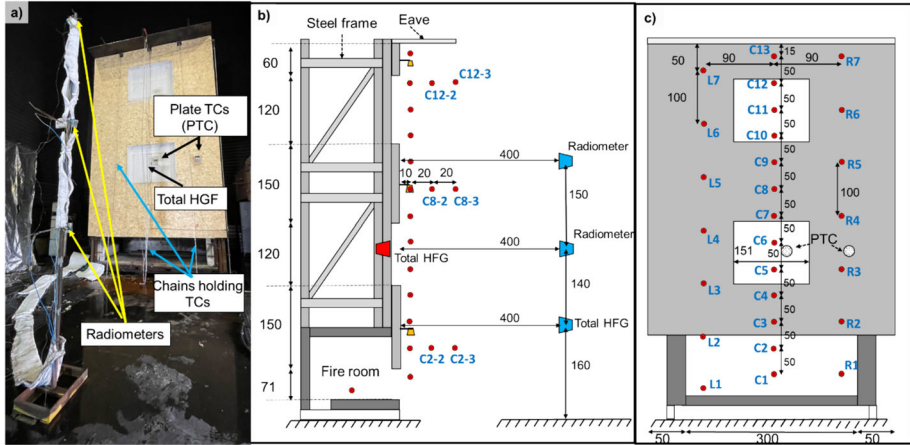
Figure 3. (a) Picture of the experimental setup, (b) Side-view at the center showing the instrumentation, (c) Front-view showing the instrumentation. All units are in cm.

The PTs were fast-response PTs, meaning a 0.05 mm thick stainless-steel foil was used instead of a solid steel plate. The foil was supported by a 1.2 mm thick steel sheet with a 50 mm diameter hole. A 0.2 mm type K thermocouple was spot-welded to the rear of the foil. The foil was backed with 20 mm insulation of type firemaster marine plus with a nominal density of 128 kg/m^3.

The incident heat flux to the PTs was determined from the temperature at the measuring point at the centre of the foil, T_p. By assuming negligible heat losses sideways and to the rear of the PT, the rate of heat stored in the steel plate per unit area, q, is proportional to the change of T_p with time, t, [11]

$$q = \rho_{st}\, c_{st}\, \delta \Delta T_p/\Delta t \tag{1}$$

where ρ_{st} is the density of the steel (8100 kg/m^3), c_{st} is the specific heat capacity of the steel (500 J/kg.K), and δ is the thickness of the steel foil (0.05 mm).

3. Results

The measurement of temperature and HFG in large-scale experiments is challenging due to high temperatures and sooty environments. Heat transfer occurs between the thermocouple and the surroundings by all the modes: conduction, convection, and radiation. The temperature measured by the thermocouple will not be the same as the actual temperature. The conduction losses can be omitted if the length of the thermocouple wire is more than 160 times its diameter [12]. In the present study, the length of the thermocouple wire is nearly 10000 mm, and the wire diameter is 1.5 mm; the ratio between the length and the diameter is nearly 6666. Therefore, the conduction losses have been omitted. The corrections

needed to obtain the actual temperature are due to convection and radiation losses. Bradley and Mathews [13] suggested that the losses due to radiation from the thermocouple can be corrected by using the following relation between the actual and the measured temperature,

$$T_g = T_t + \frac{\varepsilon_t \sigma T_t^4}{h_t} \tag{2}$$

In Equation 2, T_g represents the actual gas temperature, T_t is the temperature measured by the TC, ε_t is the emissivity of the thermocouple, σ is the Stefan-Boltzmann constant (5.67×10^{-8} W / m^2 K^4), and h_t is the heat transfer coefficient at the wire surface.

Kaskan [14] suggested that the emissivity of the thermocouple wire can be taken as a constant equal to 0.22. Bradley and Mathews [13] suggested a correlation for the convective heat transfer coefficient for the thermocouple wire surface; the correlation is given below,

$$Nu = \frac{h_t D_t}{\lambda_g} = 0.42 Pr^{0.2} + 0.57 Pr^{0.33} Re^{0.5} \tag{3}$$

where Re and Pr are the Reynolds and Prandtl numbers, respectively. The parameter λ_g is the thermal conductivity Coefficient, and it is estimated as,

$$\lambda_g = 3.75 * 10^{-5} T_t + 0.04 \tag{4}$$

The Prandtl number is estimated as follows:

$$Pr = \frac{v}{\alpha} \tag{5}$$

In Equation 5, v is the kinematic viscosity, and α is the thermal diffusivity. Temperature-dependent kinematic viscosity (v) and thermal diffusivity (α) values are obtained from a second-order polynomial fit of available data for the range of temperatures measured. The Reynolds number is calculated based on the diameter of the thermocouple wire, D_t, as,

$$Re = \frac{u D_t}{v} \tag{6}$$

u was calculated based on the theoretical plume theory developed by Baum and McCaffrey [15].

$$\frac{u}{\sqrt{g D^*}} = A \left(\frac{z}{D^*} \right)^n \tag{7}$$

z is the distance from the fuel surface and D^* is the plume scaling calculated as follows:

$$D^* = \left(\frac{\dot{Q}}{\rho_o c_p T_t \sqrt{g}}\right)^{2/5} \qquad (8)$$

where $\dot{Q}$ is the ideal heat release rate of heptane and ρ_o and c_p are the density and specific heat of air, respectively, at the measured temperature by the TC (T_t). The quantities for n and A in Equation 7 vary for each plume region and can be found in Baum and McCaffrey [15].

The equation for the convective heat transfer coefficient h_t becomes, then:

$$h_t = \frac{\lambda_g}{D_t}\left[0.42\left(\frac{v}{\alpha}\right)^{0.2} + 0.57\left(\frac{v}{\alpha}\right)^{0.33}\left(\frac{uD_t}{v}\right)^{0.5}\right] \qquad (9)$$

Water covering thermocouples is a well known challenge for suppression experiments. With the activation of the suppression system, the Pr and Re will change because the water droplets will affect the thermal diffusivity, specific heat, and velocity of the air surrounding the TC. Also, the thermocouple covered by the thin water film will not represent the gas temperature. Due to the scale of the experiments and data available, analysing the impact of water droplets on temperature measurements and determining a correction factor is challenging and falls beyond the scope of this study. In this context, corrections were only applied to the temperature data collected before the activation for the suppression tests and to the entire Freeburn test.

The time history plots presented in Figure 4 show the temperature profiles 10 cm from the façade surface for three locations: the left (90 cm from the centre), at the centre and the right side (90 cm from the centre) of the façade. In the first test (3 WM—No plates), the flames spread out of the burn chamber after 11 min and 30 s from ignition. The temperature above the burn chamber reached around 540 °C and dropped to 40 °C after the activation of the high-pressure water mist suppression system (Figure 4a). The façade temperature at the centre above the burn chamber (C3 in Figure 3) was kept below 200 °C, while the temperatures on high locations were below 20 °C for the rest of the test. The spray angle observed during the test was 50° and was not able to disperse the water droplets far enough to protect the whole façade (Figure 5a). The flame heated up the sides of the façade and caused minor damage (Figure 6b). Six percent of the façade area (excluding the windows) was charred. It was observed that the high-pressure water mist coming out from the bottom nozzle pushed the fire to the sides. The temperature on the right side, 125 cm above the burn chamber (R3), reached up to 100 °C (Figure 4b), where the OSB plates on the façade underwent slow thermal decomposition that permanently reduced their strength. The temperature profile on the left side was not measured in the first test. Additional thermocouples were
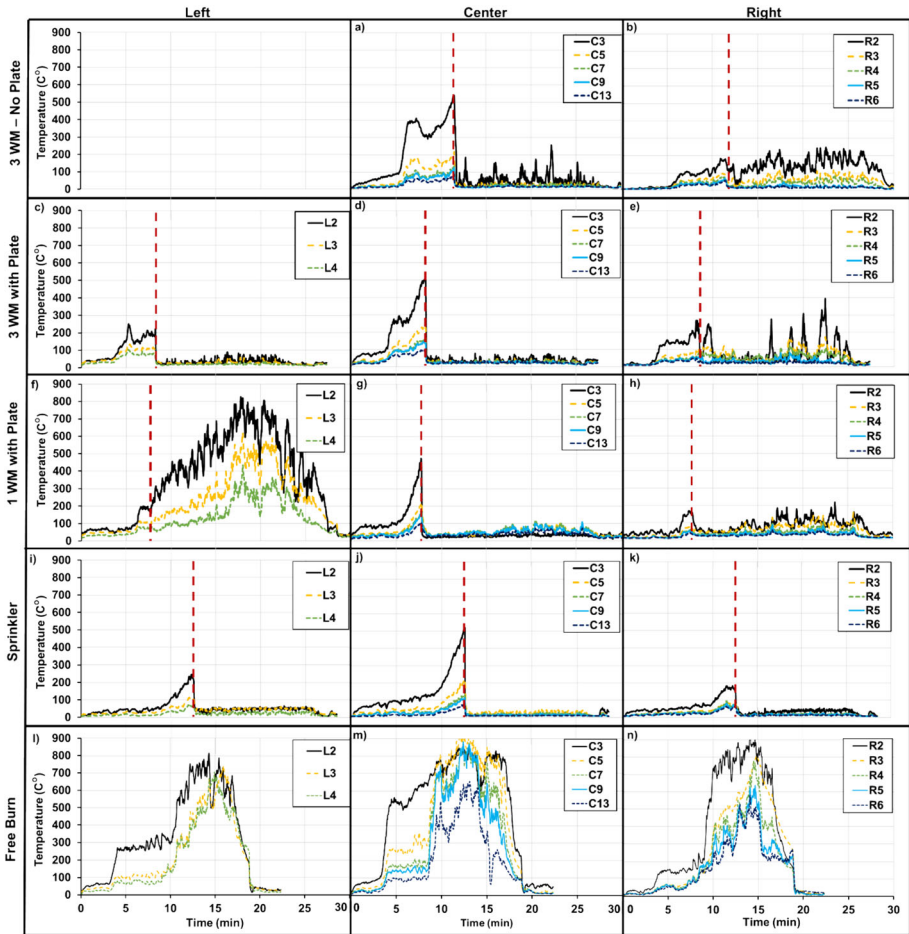
Figure 4. **Temperature measurements 10 cm away from the façade surface. (a) 3 WM—No plate, TC array at the center. (b) 3 WM—No plate, TC array on the right. (c) 3 WM with plate, TC array on the left. (d) 3 WM with plate, TC array at the center. (e) 3 WM with plate, TC array on the right. (f) 1 WM with plate, TC array on the left. (g) 1 WM with plate, TC array at the center. (h) 1 WM with plate, TC array on the right. (i) Sprinkler, TC array on the left. (j) Sprinkler, TC array at the center. (k) Sprinkler, TC array on the left. (l) Freeburn, TC array at the center. (m) Freeburn, TC array on the right. (n) Freeburn, TC array on the left. The vertical dotted line shows the activation time of the suppression system.**
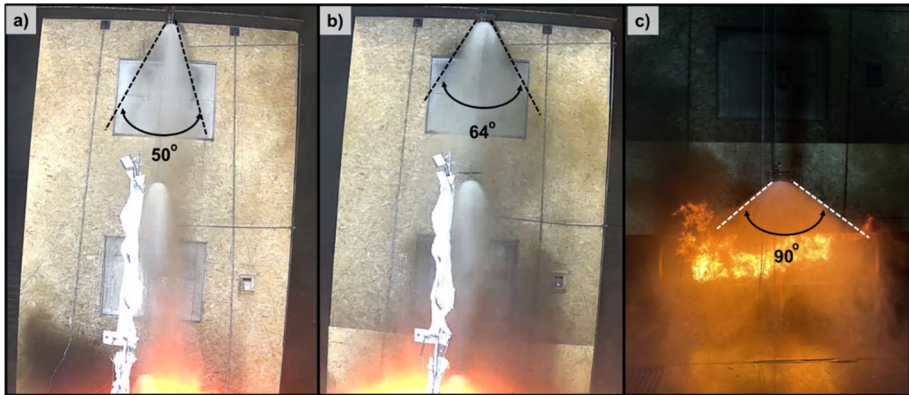
Figure 5.   Spray angle of WM nozzles. (a) No plate. (b) Plate placed 7.5 away from the nozzle head. (c) Plate placed on top of the nozzle head.

installed on the left side for all following tests to capture potential unsymmetric flame behaviour.

To disperse the water droplets further, 30 cm × 30 cm steel plates were attached 7.5 cm above the nozzle heads in the second test (Figure 2b). The flame developed faster (at 8 min 25 s after ignition) because the burn chamber was already warm from the previous test. The spray angle was measured as 64°. The modified system was able to control the heat and flame propagation for the left side and at the center (Figure 4c, d). It was observed that at 17 min of testing, the flame shifted to the right side, which caused the temperature to increase and reach above 140 °C, 125 cm above the burn chamber (R3 in Figure 4e). The charred area, 3% of the façade surface, on the right side of the façade can be seen in Figure 6c.

In the third test, the spray angle was increased to 90° by attaching the plate directly above the nozzle. After activation (at 8 min and 6 s), the flame shifted to the left and started to spread on the façade. The single nozzle effectively protected the centre but could not stop the fire after spreading to the upper parts. 5% of the façade surface burned out entirely, and 18% got damaged (Figure 6d). The sprinkler tests provided the best result in terms of minimising the damage. It acted as a water curtain and kept the façade temperature below 60 °C (Figure 4i, j, k). No damage was observed after the test (Figure 6e). A freeburn test was performed as the last test to observe the temperatures and post-fire damage without the suppression system. The flame fully developed and spread out of the burn chamber in 7 min. The façade temperatures at the centre reached 800 °C in 11 min (Figure 4m). As expected, the façade was heavily damaged. After the depletion of fuel in the burn chamber ($t = 18$ min), the fire had to be extinguished manually to protect the fire hall. 30% of the façade surface burned out, and 96% was heavily damaged (charred) (Figure 6f).

Figure 6.   Post-fire damage on the façade. (a) Pre-fire condition. (b) 3 WM. (c) 3 WM with plates. (d) 1 WM with plate. (e) Sprinkler. (f) Freeburn. Light yellow lines represent the borders of the charred areas, while yellow lines show the burned-out areas (Color figure online).

The total HFG and radiometers used in the study were calibrated with a 3% measurement uncertainty given by the calibration facility. However, the calibration was performed in a furnace emitting blackbody radiation that might lead to heat flux underestimation based on the magnitude of the convective heat flux. Kuo and Kulkarni [16] quantified this error and calculated a correction factor based on the Nusselt number correlations. This coefficient depends on the flow properties around the gauge, which was not measured in this study. Water from the suppression system brought further complications since the water droplets are expected to provide additional cooling to the case and the measuring surface. Since the gauges were actively water-cooled, the effect of the cooling of the case

would be less than that of the measuring surface. Several parameters, such as water density, droplet size, and discharged water temperature, affect the level of uncertainty. However, if the measuring surface is covered by a water film, the measured heat flux is still representative for the heat flux that a surface would be exposed to. This is not true if water is wetting the backside of a plate thermocouple, and hence, causing additional heat losses. Although, the plate thermocouples on the façade were placed in an enclosure, it is observed that the water droplets were still able to penetrate it, which affected the accuracy of the heat flux measurements. The impact of water on the plate thermocouple measurements are discussed below.

Figure 7 shows the total heat flux measured on the façade centre (i.e., in the centre of the lower window). In general, the fast-response PT shows comparable heat flux to the HFG. However, it is notable that the heat flux measured by the PT is consistently lower than that measured by the HFG once the high-pressure WM system is activated. This is only when the high-pressure WM nozzles are
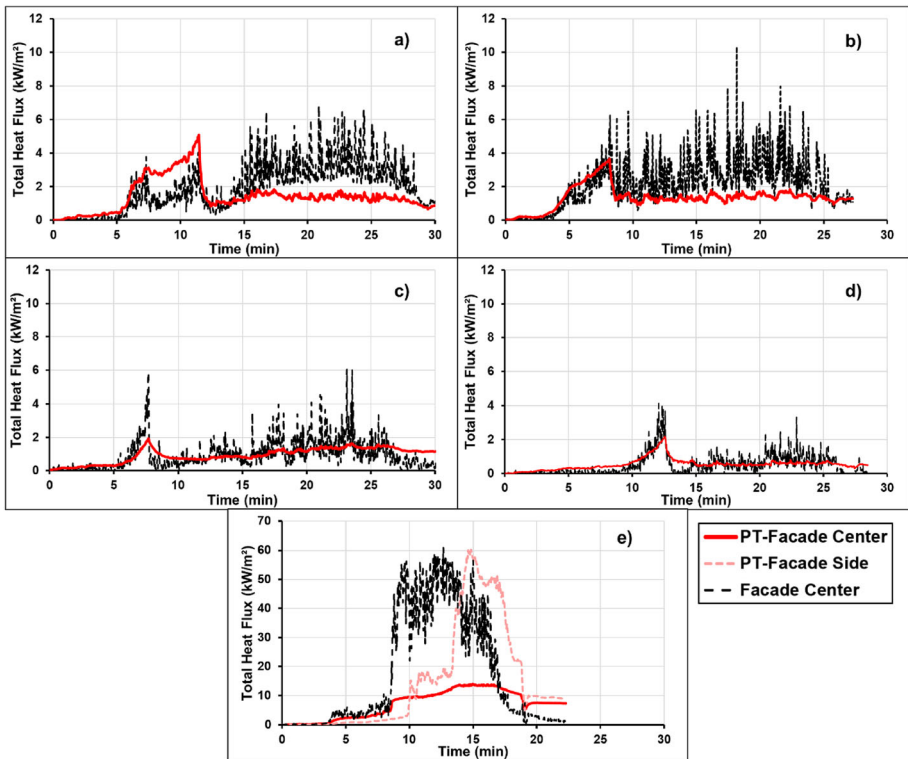

Figure 7. Heat flux measurements on the façade surface, measured by PTs (red lines) and HFG (black dashed line). (a) 3 WM—No plate. (b) 3 WM with plate. (c) 1 WM with plate. (d) Sprinkler. (e) Freeburn (Color figure online).

located above the measurement point (see Figure 7a and b), and the PT is exposed to the water mist, but not if only the high-pressure WM nozzle below is activated (see Figure 7c). The difference between the two measurement techniques is smaller in the experiment with sprinklers. One explanation could be that the larger droplets from the sprinkler nozzles are not penetrating the enclosure of the PT as easily as the small droplets from the high-pressure WM nozzles.

The PT in the centre showed a significantly lower heat flux during the Freeburn, likely caused by poor contact between the thermocouple and the steel foil (see Figure 7e). This theory is supported by the fact that the PT on the side of the façade shows a magnitude similar to that of the HFG. The trend differs due to the different positions.

All tests with an activated suppression system show very low heat fluxes on the façade, well below 12 kW/m^2, independent of the measurement technique, while the Freeburn test reached up to 60 kW/m^2 before manually extinguishing parts of the façade had to be initiated to prevent structural damage.

The heat flux data from the HFGs placed 400 cm away from the façade are presented in Figure 8. The maximum heat fluxes for the three measuring points in the Freeburn test were between 6 and 14 kW/m^2, while the heat flux was below 8 kW/m^2 for the high-pressure water mist and sprinkler tests. The heat flux measurements show that the emitted heat flux decreased with the addition of steel plates on the water mist nozzles. The lowest emitted heat flux was measured during the sprinkler test. The heat fluxes at different heights were below 1 kW/m^2.

4. Discussion

In real-life applications, a grid of nozzles needs to be used to protect the entire façade. A wider spray angle is desired for both practicality and sustainability, as it reduces material usage, the number of nozzles, and water consumption. The tests have demonstrated that a wider spray angle not only provides better protection to the sides of the façade but also results in lower temperatures in the centre of the façade, even though the same amount of water is dispersed over a larger area. All suppression systems reduced the heat flux towards the lower window by more than 90% when comparing the average heat flux over 10 min to the Freeburn. However, the system with one activated nozzle is the least robust, as the fire would, in a real scenario, be able to spread along the side past the nozzle. When the façade temperatures are compared for the cases with the same number of nozzles, both the sprinkler and the 3 WM with plate were very effective in cooling the façade. At the center at the window level, the temperature after activation was under 100 °C for both systems. The reported temperatures for façade glass breaking during extinguishing tests are usually 150 °C or higher [3]. In other words, with an early activation system, both systems will mitigate the risk of glass breakage and prevent the flame spread to the upper floors.

The radiative heat flux measured at distances of 160 and 450 cm above the ground, positioned 400 cm away from the burning façade, reached maximum values of 6 kW/m^2 and 14 kW/m^2 during the Freeburn test. The UK Building Regu-
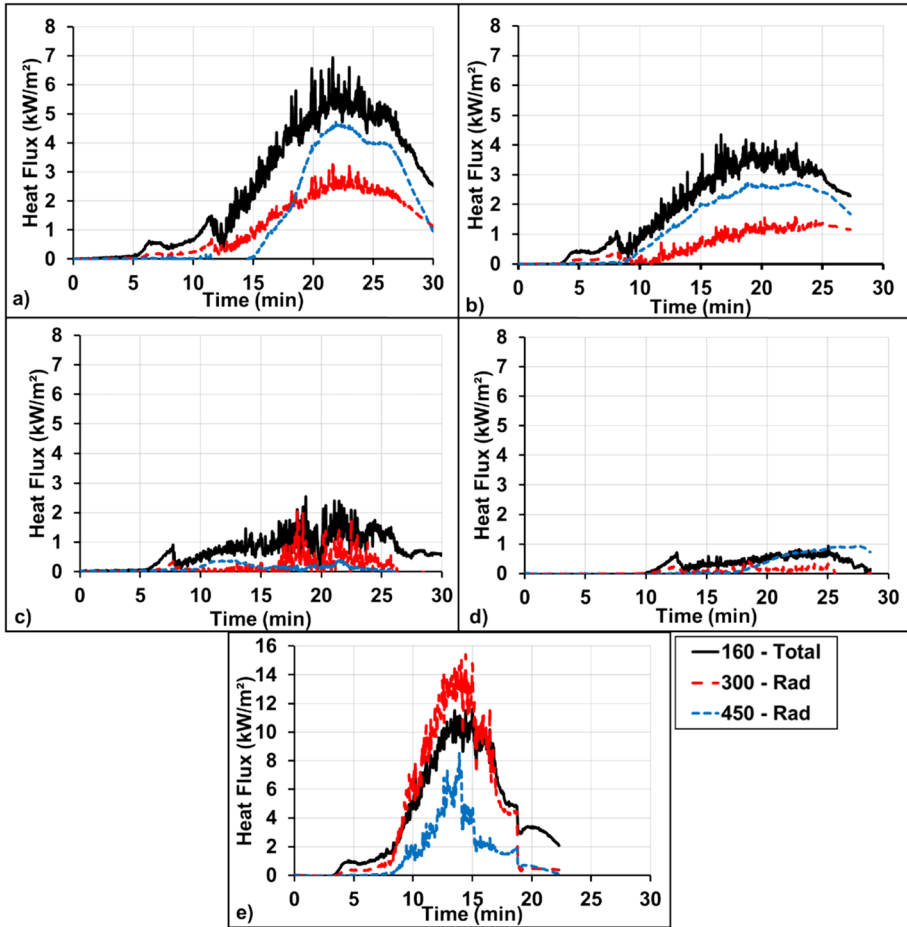
Figure 8. **Heat flux measurements 400 cm away from the façade surface at distances 160, 300 and 450 cm above the ground. (a) 3 WM—No plate. (b) 3 WM with plate. (c) 1 WM with plate. (d) Sprinkler. (e) Freeburn.**

lations use a minimum heat flux for ignition of combustible building materials of 12.6 kW/m^2, which has been obtained through experimentation of small samples of wood heated in a cone calorimeter [17]. The Dutch building regulations uses 15 kW/m^2 as the critical heat flux for wood and synthetic materials. All tested suppression systems were able to reduce the measured heat flux below these levels. Without a suppression system, continuous exposure to radiation may cause the remote ignition of adjacent façades made from wood or synthetic materials. Prolonged exposure to radiation may also cause life-threatening conditions, severe burns at 5 kW/m^2 with 20 s exposure, or fatality above 25 kW/m^2 in 1 min [18].

The results show that for the test setup of this work, the sprinklers were the most effective in damage protection and reducing the heat flux to the surround-

ings. Depending on the height, between 87 and 98% of the incident flux measured 400 cm from the façade was attenuated by the sprinkler system. The single nozzle WM system achieved a comparable attenuation of 84 to 98%. The narrow spray angle of the three nozzle WM systems, with and without plate, caused a more heterogenous heat flux reduction. At a height of 3 m, the reduction was 75 to 92%, respectively, while the reduction at a height of 4.5 m was only 27 and 30%. However, as the test with a single activated nozzle showed, this can be improved by adequately designing the spray angle.

While the effectiveness in protecting adjacent constructions was comparable between the WM and the sprinkler systems, the efficiency for the WM systems was higher, considering the water consumption. The high-pressure WM system with a single nozzle reduced the heat flux at 400 cm from the façade during 10 min on average (over height) by 2.18 J/m^2 per litre of water used, while the reduction by the sprinkler system was 0.19 J/m^2 per litre of water used. Hence, the high-pressure WM system was almost 12 times as efficient. Assuming a system with three nozzles but a wide spray angle would have the same effectiveness as the WM system with one nozzle, the efficiency would still be 3.8 times higher than the sprinkler system's efficiency. This means the smaller WM droplets with high surface area effectively extract the energy from the fire. For areas where fresh water is becoming a scarcer resource, extinguishing systems with more nozzles and lower water usage can be more attractive than sprinkler systems with high water consumption. However, it is important to consider that neither tested system was optimised for the setup and wind conditions were not considered.

The operating pressures given by the manufacturers for the sprinkler and the high-pressure water mist system are 0.35 bar–12 bar and 100 bar–140 bar, respectively. In the present study, 1.8 bar and 100 bar were selected for the sprinkler and WM, resulting in 107.3 L/min/nozzle and 27.4 L/min/nozzle, respectively. If the sprinkler system had operated with the lowest operating pressure, that would have resulted in 47.3 L/min/nozzle. This means the sprinkler system was operated with a potential safety factor of up to 2.2, while it was 1 for WM. Hence, even with the lowest operation pressure, without any safety factors, the sprinkler system would have used 1.7 times more water than the WM system in Test 1 and Test 2, and 5.2 times more than Test 3.

Recent studies [19–21] have shown that wind speed and direction play a significant role in the spread of facade fires. At high speeds, the lateral winds can promote lateral fire spread, while diagonal winds can cause the fire to spread faster vertically and even penetrate the space between the facade and the structural components. Although the impact of wind on façade fires is well known, the interaction between wind, fire, and water is yet to be investigated in detail. This interaction has been investigated in tunnel fire suppression studies. Liu et al. [22] studied the individual and combined effect of a water mist system and longitudinal ventilation on the fire HRR, smoke temperature, and back-layering. It was demonstrated that when the water mist and ventilation were applied individually, the HRR was reduced. However, under the combined conditions, the HRR reduced first and then increased again when the ventilation speed was increased. The reduction occurred due to high wind speed, which carried the water droplets

away, resulting in less water in the flame region to attenuate the fire. Crosfield et al. [23] developed a model to calculate the landing distances of water mist droplets with different diameters under various ventilation flows and conditions common in modern tunnels. The results showed that with a 3 m/s ventilation flow, water droplets from 90 to 170 μm in diameter released from a suppression system placed 6 m high carried between 60 and 130 m downstream before reaching the ground. Larger droplets, 300 μm in diameter, landed 20–25 m away for 3 m/s.

The distances between the nozzles and the burn chamber are given in Table 1. According to Crosfield et al. [23], at 3 m/s wind speed, the water mist droplets used in this study (with 90–100 μm diameter) were expected to be carried away between 0–2 m, 20–50 m, and 90–140 m downstream for the bottom, middle and top nozzles, respectively. For the sprinkler system, the wind would have minimal impact on the water droplets due to large droplet size and short distance between the nozzle and the burn chamber. In real-life applications, the nozzle configuration and the vertical distance between the nozzle and the window need to be determined based on the wind speed and the droplet size.

5. Conclusions

A series of large-scale façade fire experiments were conducted using an SP Fire 105 setup covered with oriented strand boards (OSB) to study the influence of sprinklers and high-pressure water mist (WM) systems on the temperature, heat flux, flame spread and postfire damage. Three high-pressure WM tests were performed with different spray angles (50°, 64° and 90°) and number of activated nozzles (1 and 3). The spray angle was changed by adding a square steel plate above the nozzle at different distances. The results were compared with a sprinkler system. A freeburn test was performed at the end to obtain baseline data. Novel fast-response plate thermocouples (PTs) were mounted on the façade. The heat flux measured by the relatively simple PTs showed good agreement with the measurement by a water-cooled heat flux gauge. However, the PTs appeared more sensitive to water from the suppression systems.

The results demonstrated the importance of a sufficiently wide spray angle to ensure cooling of the façade's far sides. For the test with the same number of high-pressure WM nozzles, a wider spray angle decreased the damage on the façade. The wider angle also reduced the measured heat flux 400 cm from the facade on average by 44 and 59%, respectively. The test with a single high-pressure WM nozzle placed above the combustion chamber effectively suppressed the temperature at the centre and was the most efficient concerning water consumption. The single high-pressure nozzle system is, however, not robust, as the flame was able to spread on the side of the façade. The sprinkler system was the most effective in controlling the façade temperature, the vertical and horizontal flame spread, and the heat flux. However, the sprinkler was the least efficient system as the water consumption was four times larger than the consumption of the high-pressure WM system with three nozzles. The large droplets formed streams of water running down a façade. The sprinkler system attenuated, on average, 98%

of the incident flux onto the façade compared to the Freeburn. No damage was observed after the fire. During the Freeburn, the façade temperature and the emitted heat flux 400 cm from the façade reached up to 900 °C and 15 kW/m^2, respectively, which may cause the self-ignition of wood and synthetic materials on the nearby buildings. This study demonstrates that both the sprinkler and high-pressure WM systems can reduce the risk of fire spreading on the façade and between buildings. The efficiency of the high-pressure WM systems can be optimised by changing the nozzle alignment, but the effect of wind on the droplet dispersion should be further investigated since the less water required by the high-pressure water mist system is attractive, seen from a sustainable perspective.

The present study is based on only a few experiments, all with similar ventilation conditions and the same nozzle placement in relation to the fire source. Further experimental work should, therefore, be conducted to derive more robust conclusions.

Funding

Open Access

References

1. Kim AK, Taber BC, Lougheed GD (1998) Sprinkler protection of exterior glazing. Fire Technol 34(2):116–138. https://doi.org/10.1023/A:1015325418666
2. Gui J et al (2019) Full-scale experimental study on the suppression effect of water sprinkler system on energy saving building fire. IOP Conf Ser Earth Environ Sci 354(1):012096. https://doi.org/10.1088/1755-1315/354/1/012096
3. Węgrzyński W, Antosiewicz P, Burdzy T, Tofiło P, Papis BK (2020) Experimental investigation into fire behaviour of glazed façades with pendant type sprinklers. Fire Saf J 115:103159. https://doi.org/10.1016/j.firesaf.2020.103159
4. NFPA "NFPA 750 Standard on Water Mist Fire Protection Systems," NFPA (2019)
5. Yang W, Parker T, Ladouceur HD, Kee RJ (2004) The interaction of thermal radiation and water mist in fire suppression. Fire Saf J 39(1):41–66. https://doi.org/10.1016/j.firesaf.2003.07.001
6. Parent G, Morlon R, Acem Z, Fromy P, Blanchard E, Boulet P (2016) Radiative shielding effect due to different water sprays used in a real scale application. Int J Therm Sci 105:174–181. https://doi.org/10.1016/j.ijthermalsci.2016.02.008
7. Collin A, Lechene S, Boulet P, Parent G (2010) Water mist and radiation interactions: application to a water curtain used as a radiative shield. Numer Heat Transf Part Appl 57(8):537–553. https://doi.org/10.1080/10407781003744722
8. Fisher BT, Awtry AR, Sheinson RS, Fleming JW (2007) Flow behavior impact on the suppression effectiveness of sub-10-μm water drops in propane/air co-flow non-premixed flames. Proc Combust Inst 31(2):2731–2739. https://doi.org/10.1016/j.proci.2006.07.023
9. SP FIRE 105. External wall assemblies and façade claddings. Reaction to fire. Swedish National Testing and Research Institute, Fire Technology, Borås, Sweden, Sep 09, 1994
10. ISO 6182-1 Fire protection—automatic sprinkler systems—part 1: requirements and test methods for sprinklers (2021)
11. Ingason H, Wickström U (2007) Measuring incident radiant heat flux using the plate thermometer. Fire Saf J 42(2):161–166. https://doi.org/10.1016/j.firesaf.2006.08.008
12. Moneib HA (1980) Experimental study of the fluctuating temperature in inert and reacting turbulent jets, Imperial Collage of Science and Technology
13. Bradley D, Mathews KJ (1968) Measurement of high gas temperatures with fine wire thermocouples. J Mech Eng Sci 10(4):299–305. https://doi.org/10.1243/JMES_JOUR_1968_010_048_02
14. Kaskan WE (1957) The dependence of flame temperature on mass burning velocity. In: 6th symposium (international) on combustion. The Combustion Institute, Pittsburgh, pp. 34–143
15. Baum HR, McCaffrey BJ (1989) Fire induced flow field-theory and experiment. In: Proceedings of the second international symposium on fire safety science, New York, USA, pp 129–148
16. Kuo CH, Kulkarni AK (1991) Analysis of heat flux measurement by circular foil gages in a mixed convection/radiation environment. J Heat Transf 113(4):1037–1040
17. Burrell G, Hare J (2006) Review of HSE building ignition criteria. Health & Safety Laboratory, Fire and Explosion Science Group, Derbyshire, UK, HSL/2006/33
18. LaChance J, Tchouvelev A, Engebo A (2011) Development of uniform harm criteria for use in quantitative risk analysis of the hydrogen infrastructure. Int J Hydrog Energy 36(3):2381–2388

19. Abu-Zidan Y, Rathnayaka S, Mendis P, Nguyen K (2022) Effect of wind speed and direction on facade fire spread in an isolated rectangular building. Fire Saf J 129:103570
20. Fang X, Ren F, Zhang X, Sun X, Yang Y, Hu L (2020) Facade flame height ejected from opening of a compartment under the coupling effect of side walls and ambient wind. Fire Saf J 112:102966
21. Hu L, Hu K, Ren F, Sun X (2017) Facade flame height ejected from an opening of fire compartment under external wind. Fire Saf J 92:151–158
22. Liu Y, Fang Z, Tang Z, Beji T, Merci B (2021) The combined effect of a water mist system and longitudinal ventilation on the fire and smoke dynamics in a tunnel. Fire Saf J 122:103351
23. Crosfield R, Cavallo A, Colella F, Carvel R, Torero J, Rein G (2009) Approximate travelling distances of water mist droplets in tunnels. Presented at the International Water Mist Conference, London, UK, Sep 2009